Bioconjugate Chemistry

Article

pubs.acs.org/bc

Star-Like Oligo-Arginyl-Maltotriosyl Derivatives as Novel Cell-Penetrating Enhancers for the Intracellular Delivery of Colloidal Therapeutic Systems

Sara Bersani, Stefano Salmaso, Francesca Mastrotto, Elena Ravazzolo, Alessandra Semenzato, and Paolo Caliceti*

Deprtament of Pharmaceutical and Pharmacological Sciences, University of Padova, Via F. Marzolo, 5 35131 Padova, Italy

ABSTRACT: A novel nonpeptide, multiarmed oligo-arginyl derivative was engineered as a cell-penetration enhancer for the delivery of bioactive macromolecules and colloidal drug systems. Hepta-arginyl-maltotriosylamido-*N*-acetyl-dodecanoyl acid (Arg_7-Malt-$NAcC_{12}$ acid) was synthesized through a carefully designed multistep chemical protocol, as follows: (1) maltotriose derivatization with 12-amino-dodecanoic acid and acetylation of the free amino group; (2) esterification of the maltotriosyl hydroxyl groups with 2-bromo-isobutyryl bromide; and (3) synthesis of star-like oligomer bearing multiple copies of arginine moieties under atom transfer radical polymerization (ATRP) conditions. The intermediates and final product were characterized by ^{1}H NMR, IR, mass spectrometry, colorimetric assays, and elemental analysis. Cytotoxicity studies on the final polymeric material showed that this novel cell-penetrating enhancer does not have significant toxic effects on MCF-7 and MC3T3-E1 cell lines. The IC_{50} was greater than 100 μM with both cell lines, while the polyethylenimine with similar average molecular mass (M_n) that was used as a reference showed an IC_{50} of 30 and 40 μM, for MCF-7 and MC3T3-E1, respectively. The biological properties of the novel bioconjugate were investigated using a fluorescein-labeled bovine serum albumin (FITC-BSA) as a hydrophilic cargo model. MCF-7 and MC3T3-E1 cells were incubated for 60 min with the Arg_7-Malt-$NAcC_{12}$-conjugated FITC-BSA [$(Arg_7$-Malt-$NAcC_{12})_2$-FITC-BSA] or FITC-BSA, and the intracellular fluorescence level was analyzed by spectrofluorimetric analysis of cell lysate, cytofluorimetry, and confocal microscopy. The fluorescence of the lysate of MCF-7 and MC3T3-E1 cells that were incubated with $(Arg_7$-Malt-$NAcC_{12})_2$-FITC-BSA at 37 °C was approximately 4.5 times higher than the fluorescence obtained with cells incubated with FITC-BSA. At 4 °C, the cell uptake of $(Arg_7$-Malt-$NAcC_{12})_2$-FITC-BSA was only 2 times higher than that of FITC-BSA. Cytofluorimetric studies showed that, after $(Arg_7$-Malt-$NAcC_{12})_2$-FITC-BSA treatment, over 80% of MCF-7 cells and over 95% of MCF-7 cells displayed enhanced fluorescence. Confocal investigations showed punctuated fluorescence within the cytosol in both cell lines, indicating that $(Arg_7$-Malt-$NAcC_{12})_2$-FITC-BSA was confined to endosomes, with no fluorescence observed in the nucleus.

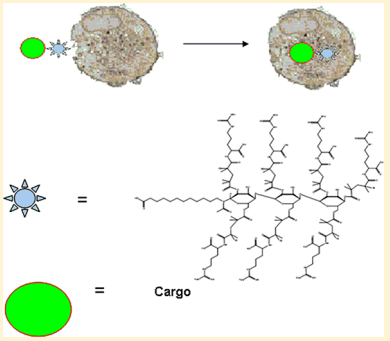

INTRODUCTION

The impermeable nature of large hydrophilic structures to biological barriers is one of the primary causes for the poor absorption and inefficient intracellular delivery of proteins, oligonucleotides, and colloidal supramolecular systems. Poor transmembrane permeability strongly limits the development of efficient, nonparenteral formulations, and the intracellular delivery of bioactive macromolecules and colloidal therapeutic systems, such as polymer conjugates and nanoparticles.[1] The development of technologies that enable low-membrane-permeability therapeutics to effectively penetrate biological membranes is currently one of the greatest challenges in pharmaceutical development.[2]

Recently, small regions of proteins, termed protein transduction domains (PTDs) or cell-penetrating peptides (CPPs), have been demonstrated to possess cell-penetrating properties that can be exploited to enhance the performance of colloidal therapeutics.[3−6]

CPPs include Tat (trans-activator of transcription)-derived peptides, signal sequence-derived peptides, and synthetic or chimeric peptides. Most of the recognized CPPs contain cationic, amphiphilic, or hydrophobic functions that promote cell surface interaction and translocation.

Tat-derived peptides have been demonstrated to be very efficient penetrating agents. Synthetic peptides have been designed to mimic the HIV-1 Tat structure, an 86-amino-acid nuclear transcription-activating protein comprising three functional domains. The region responsible for cell uptake and nuclear import contains 6 arginine and 2 lysine residues within a short linear sequence, and the amino acids are in random conformation.[7]

The presence of short peptide sequences containing basic residues, such as arginines and lysines, is a structural requisite to enabling cell-penetrating activity and nucleus translocation of these oligo amino acids.[8,9] Accordingly, model peptides that contain repeat motifs or poly residues, such as homopolymers

Received: January 3, 2012
Revised: May 4, 2012

   dx.doi.org/10.1021/bc200666u | *Bioconjugate Chem.* XXXX, XXX, XXX−XXX

of arginine, have been synthesized and investigated. Studies have demonstrated that their internalization efficiency depends on the length of the peptide backbone. Stretches of six (R6) to eight (R8) arginine residues showed the highest cytoplasmic internalization ability.[10]

The exact mechanism by which cell translocation occurs is still a matter of debate, as either passive or active pathways, or receptor- or absorptive-mediated endocytosis, have been proposed. In addition, the correlation between the structural features of these peptides and the cell uptake behavior is still under investigation.[11,12]

Although many aspects of CPP activity have not been fully elucidated, and a number of contrasting data have been generated, it is anticipated that these molecules will have a broad relevance in the pharmaceutical and medical fields, and they may find applications either for enhancing transmucosal absorption, mostly for nasal and intestinal delivery, or for intracellular drug delivery and targeting.[13,14] Covalent linkages or simple physical interactions of CPPs have been demonstrated to promote the cell entry of a variety of hydrophilic compounds ranging from small molecules to plasmid DNA and oligonucleotides,[15,16] peptides,[17,18] proteins,[19−21] nanocarriers, such as liposomes and micelles,[22] and quantum dots.[23,24] Nevertheless, many studies have highlighted pitfalls in using CPPs in drug delivery, including poor cell uptake, unspecific cell delivery, inconvenient *in vivo* performance, low stability, and intrinsic biological activity. Therefore, the use of these molecules in combination with colloidal therapeutic systems may result in ineffective systems and/or entail risks of toxicity.[25]

These drawbacks could be overcome by designing novel nonpeptide molecules with cell-penetrating activity. These novel structures could display higher stability and lower toxicity compared to CPPs and may be devoid of intrinsic biological activity. Recently, high-molecular-weight polymers bearing oligo-Arg as pendant functions have been demonstrated to enhance the nasal absorption of insulin.[26] Oligo-Lys and oligo-Arg hydrophobic-core polysaccharide dendrons have been investigated for the oral delivery of heparin.[27] A novel class of Arg-rich dendrimers has been successfully developed for the conjugation and delivery of PNA705 splice-redirecting oligonucleotides,[28] while a myristoylated hendecaarginine derivative has been found to possess promising cell-penetration properties for pharmaceutical applications.[29]

Intrigued by the evidence that nonpeptide cell-penetrating enhancers may be advantageously exploited for drug delivery, we designed a novel class of cell-penetrating enhancers with unusual star-like structures that can be covalently or physically combined with colloidal therapeutic systems to promote their cellular uptake. The new enhancers were designed with regard to the oligo-Arg structure of the Tat-penetrating domain 49−57 and the evidence that the guanidinium headgroup of Arg are crucial for cellular uptake due to their interactions with membrane phospholipids.[30] Guanidinium-rich structures, in fact, undergo cell translocation three times faster than the transduction domain of Tat, as their insertion into lipid bilayers produces local membrane distortion leading to transient pore formation on the membranes.[31]

In this paper, we report an efficient, multistep protocol for the synthesis of a novel nonlinear multi-Arg-armed molecule starting from a short oligosaccharide. The cell-penetration properties of the multiarmed derivative were investigated using fluorescein-labeled bovine serum albumin as a hydrophilic cargo model. The cell-penetration studies were performed using two cell lines and fluorescence spectroscopy, flow cytofluorimetry, and confocal microscopy.

MATERIALS AND METHODS

Maltotriose [*O*-α-D-glucopyranosyl-(1,4)-*O*-α-D-glucopyranosyl-(1,4)- α-D-glucopyranose], 12-amino-dodecanoic acid, acetic anhydride, 2-bromo-isobutyryl bromide, triethylamine, ascorbic acid, 1-ethyl-3-(3-dimethylaminopropyl) carbodiimide hydrochloride (EDC), polyethylenimine (PEI, 1.8 kDa Mn), fetal bovine serum (FBS), RPMI-1640 medium, Dulbecco's modified essential medium (D-MEM), penicillin (10 000 IU/mL)−streptomycin (10 mg/mL)−amphotericin B (25 μg/mL) stabilized solution, L-glutamine (200 mM), Dulbecco's phosphate buffered saline (DPBS), trypsin−EDTA solution (2.5 w/v %), and 3-(4,5-dimethylthiazol-2-yl)-2,5-diphenyltetrazolium bromide (MTT) were purchased from Sigma-Aldrich (St. Louis, MO, USA). L-Arginine hydrochloride was furnished by SERVA Electrophoresis (Heidelberg, Germany). Fluorescein isothiocyanate (FITC), 2-picolyl hydrochloride, 2-picolylamine, copper(I) bromide (CuBr), bovine serum albumin−fraction V (BSA), Triton X-100, and paraformaldehyde were purchased from Fluka (Buchs SG, Switzerland). Vectashield Mounting Medium with DAPI was from Vector Laboratories (Peterborough, UK). All other reagents were obtained from Fluka Analytical or Sigma-Aldrich. The solvents of analytical or HPLC grade were furnished by Carlo Erba (Milan, Italy), VWR International (Lutterworth, UK), and Sigma-Aldrich (St. Louis, MO, USA). Cell culture plates and flask, 96-well flat bottomed microassay plate and chambered slides were purchased from BD Falcon (BD Bioscience, NJ, USA).

Synthesis of Maltotriosylamido-*N*-Acetyl-Dodecanoic Acid (Malt-NAcC_{12} acid). 12-Amino-dodecanoic acid (1.0 g, 4.6 mmol) was dissolved in 15 mL of methanol/acetic acid (95:5 vol/vol). The solution was maintained at 60 °C, and 1.2 g of maltotriose (2.4 mmol) was added. After 24 h, 7.5 mL of acetic anhydride (79.4 mmol) was added, and the resulting solution was stirred for 96 h at room temperature. The volume was reduced to ca. 4 mL under vacuum, and then 3 mL of 30% ammonia aqueous solution was added. After 12 h, the solvent was removed under reduced pressure, and the crude product was redissolved in 3 mL of methanol and added dropwise to 200 mL of diethyl ether. The precipitate was collected by filtration and desiccated under vacuum. The recovered product mass was 1.2 g. The product was analyzed by RP-HPLC using a Luna C18 column (250 × 4.6 mm, Phenomenex, Torrance, CA, USA) eluted with a gradient of H_2O/0.05% trifluoroacetic acid (A) and acetonitrile/0.05% trifluoroacetic acid (B) (0−3 min 10% B, 3−27 min from 10% to 80% B). The UV detector was set at 220 nm. The product was also characterized by elemental analysis, mass spectrometry (ESI-MS; ESI-TOF Applied Biosystems Mariner Foster City, CA, USA), ^{1}H NMR (AMX 300 MHz, Bruker Spectrospin, Fallanden, Switzerland), and FT-IR (FT-IR 1600, Perkin-Elmer, Norwalk, CT, USA).

RP-HPLC (C18): 16.3 min retention time. Elemental analysis: C, 51.2%; H, 7.9%; N, 1.7% (O, 39.2%) [calcd for Malt-NAcC_{12} acid ($C_{32}H_{57}NO_{18}$): C, 51.7%; H, 7.7%; N, 1.8% (O, 39.8%)]. ESI-MS [*m*/*z*]: 742.34 $(M\text{-}H^+)^{1-}$ [calcd for $C_{32}H_{57}NO_{18}$: 743.36]. ^{1}H NMR (D_2O): δ ppm 5.40 (d, *J* = 3.3 Hz, 2H, anomeric), 5.23 (d, *J* = 3.8 Hz, 1H, anomeric), 4.20−3.60 (m, 18H - sugar region), 3.55 (t, *J* = 9.3 Hz, 2H, λ-CH_2−), 2.33 (t, *J* = 7.2 Hz, 2H, α-CH_2−), 2.18 (s, 3H, CH_3−CO−), 1.59 (bm, 4H, ι-CH_2− and β-CH_2− of alkyl chain), 1.29 (bs,

dx.doi.org/10.1021/bc200666u | *Bioconjugate Chem.* XXXX, XXX, XXX−XXX

14H, $-CH_2-$ of alkyl chain). NMR signals were indicated as singlet (s), broad singlet,[32] doublet (d), triplet (t), multiplet (m), and broad multiplet (bm); coupling constants of peak multiplicities (J) have been expressed in Hz. FT-IR (KBr): ν (cm^{-1}) 3396 (OH), 2929 (CH), 1717 (CO−OH), 1612 (acetyl CO−N).

Synthesis of Hepta(2-bromoisobutyryl)-Maltotriosylamido-*N*-Acetyl-Dodecanoic Acid (BrIsoBut$_7$-Malt-NAcC$_{12}$ acid). Hepta(2-bromoisobutyryl)-maltotriosylamido-*N*-acetyl-dodecanoic acid (BrIsoBut$_7$-Malt-NAcC$_{12}$ acid) was synthesized according to a modified procedure reported in the literature.[33] Briefly, 1.0 g of Malt-NAcC$_{12}$ acid (1.35 mmol) was suspended in 20 mL of anhydrous chloroform containing triethylamine (3.7 mL, 26.7 mmol). The suspension was cooled to 0 °C, and 2-bromo-isobutyryl bromide (3.3 mL, 26.7 mmol) was added over 30 min. The solution was stirred for 72 h. The mixture was filtered, and the organic solution was washed three times with 30 mL of cold water, three times with 20 mL of 0.1 N NaOH, and again three times with 30 mL of cold water. The organic phase was then dried over anhydrous Na_2SO_4, filtered, and concentrated under reduced pressure. The resulting red−brown solid was dissolved in 5 mL of acetone and added to 100 mL of cold water under vigorous stirring. Acetone was removed under reduced pressure, and the aqueous suspension was lyophilized. The crude product (1.47 g) was analyzed by elemental analysis, ^{1}H NMR, and FT-IR.

Elemental analysis: C, 40.8%; H, 5.1%; N, 1.0%; Br, 30.4% (O, 22.7%) [calcd for BrIsoBut$_7$-Malt-NAcC$_{12}$ acid ($C_{60}H_{92}Br_7N_1O_{25}$): C, 40.3%; H, 5.2%; N, 0.8%; Br, 31.3% (O, 22.4%)]. ^{1}H NMR ($CDCl_3$): δ ppm 4.60−3.30 (m, 18H sugar region), 3.29 (m, 2H, λ-CH_2-), 2.15 (m, 2H, α-CH_2-), 1.96 (bs, 42H, CH_3), 1.94 (s, 3H, CH_3-COO-), 1.59 (m, 4H, ι-CH_2- and β-CH_2- of alkyl chain), 1.33−1.22 (bm, 14H, $-CH_2-$ of alkyl chain). FT-IR: ν (cm^{-1}) 3437 (OH), 2932 (CH), 1743 (isobutyryl CO-O), 1619 (acetyl CO-N).

Synthesis of Arginine-Methacryloylamide (Arg-methacryloylamide). Arginine-methacryloylamide (Arg-methacryloylamide) was synthesized according to a procedure described in literature.[34] Arginine hydrochloride (2.1 g, 10 mmol) was dissolved in 20 mL of saturated $NaHCO_3$ solution and was then cooled to 0 °C. Next, 970 μL of methacryloyl chloride (10 mmol) was added dropwise under vigorous stirring. After 1 h, the pH of the mixture was adjusted to 1 with hydrochloric acid, and the solution was saturated with sodium chloride, filtered, washed three times with 30 mL of ethyl acetate, and finally extracted three times with 20 mL of a 1:1 vol/vol mixture of ethyl acetate/isopropanol. The ethyl acetate/isopropanol fractions were pooled, concentrated under reduced pressure, and filtered. The resulting colorless oil was added to 50 mL of water, and the resulting solution was freeze−dried. The mass of the final product was 2.4 g. The product was analyzed by ESI-MS, ^{1}H NMR, and FT-IR.

ESI-MS [m/z]: 243.13 ($M+H^+$) [calcd for Arg-methacryloylamide ($C_{10}H_{18}N_4O_3$): 242.14]. ^{1}H NMR (D_2O): δ ppm 5.69 (s, 1H, HHC═C), 5.47 (s, 1H, HHC═C), 4.41 (dd, J = 9.2, 5.1 Hz, 1H, α-CH), 3.20 (t, J = 6.8, 2H, δ-CH_2), 1.91 (s, 3H, CH_3), 1.85−1.72 (m, 2H, γ-CH_2), 1.72−1.58 (m, 2H, β-CH_2). FT-IR (KBr): ν (cm^{-1}) 3368 (OH), 3150 ($NHC(NH_2)_2^+$), 1654 (C═C, C═O, and C═N), 1528 (CNH_2 or CNH_3^+).

The purity of the compound was assessed by the integration of the ^{1}H NMR triplet at 3.20 ppm compared with methacryloyl singlets at 5.69 and 5.47 ppm (99%).

Synthesis of Tris[(2-pyridyl)methyl]amine (TPMA). Tris[(2-pyridyl)methyl]amine (TPMA) was prepared according to a modified protocol described in the literature.[32] First, 2-picolyl chloride (10.0 g, 61.0 mmol) was dissolved in 25 mL of distilled water, and the mixture was cooled to 0 °C and added to 12 mL of 5 N NaOH. This solution was then added to 2-(aminomethyl)pyridine (3.2 mL, 30.5 mmol) and 50 mL of dichloromethane. The reaction mixture was allowed to reach room temperature under vigorous stirring and the pH was maintained at 9.5 by the addition of 5.0 N NaOH. After 48 h, the organic phase was washed three times with 20 mL of 2.5 N NaOH and then dried with anhydrous Na_2SO_4 and filtered. The organic solvent was removed under reduced pressure. TPMA was recovered by extracting the resulting waxy, red−brown residue three times with 25 mL of boiling petroleum ether. The volatiles were removed under vacuum to afford the desired TPMA ligand. The mass of the final product was 5.6 g.

ESI-MS [m/z]: 291.15 $(M+H^+)^{1+}$ and 313.14 $(M+Na^+)^{1+}$ [calcd for TPMA ($C_{18}H_{18}N_4$): 290.15]. ^{1}H NMR ($CDCl_3$): δ ppm 8.53 (d, J = 4.2 Hz, 3H, H-α), 7.65 (t, J = 7.6 Hz, 3H, H-$\beta\delta$), 7.6 (d, 3H, H-$\beta\delta$), 7.1 (t, 3H, H-γ), 3.9 (s, 6H, $-CH_2-$).

Synthesis of Hepta-Arginyl-Maltotriosylamido-*N*-Acetyl-Dodecanoic Acid (Arg$_7$-Malt-NAcC$_{12}$ acid). TPMA (1.31 g, 4.5 mmol), CuBr (0.65 g, 4.5 mmol), and ascorbic acid (7.9 mg, 0.045 mmol) were dissolved in 5 mL of DMSO that had been previously purged with nitrogen. This solution was then added to 8.5 mL of 0.18 mg/mL Arg-methacryloylamide solution (6.3 mmol) in DMSO while stirring at 55 °C. Next, the solution was added to 3 mL of 0.27 mg/mL BrIsoBut$_7$-Malt-NAcC$_{12}$ acid (0.45 mmol) in DMSO. The reaction mixture was maintained under an atmosphere of nitrogen for 12 h and then was exposed to air. Next, the solution was added dropwise to 200 mL of an ice-cold 1:1 acetone/diethyl ether mixture containing 1% acetic acid. The precipitate was desiccated under reduced pressure, redissolved in 5 mL of warm methanol, and reprecipitated by the addition of the resulting solution into 200 mL of the acetone/diethyl ether/acetic acid mixture. Using this procedure, we obtained 1.54 g (98% product yield) of Arg$_7$-Malt-NAcC$_{12}$ acid. The arginine content in the final product was quantified by Sakaguchi assay.[35] The experimental data were plotted on a calibration curve obtained with standard solutions of 0−0.6 μM guanidinium content (y = 7.3955x − 0.0386, R^2 = 0.99). The final product was also analyzed by elemental analysis, FT-IR, and ^{1}H NMR (D_2O).

Elemental analysis: found C, 39.3%; H, 5.9%; N, 10.0%; Br, 28.1% (O, 16.7%); [calcd for Arg$_7$-Malt-NAcC$_{12}$ acid HBr salt ($C_{130}H_{218}Br_7N_{29}O_{46}$·7HBr): C, 38.6%; H, 5.6%; N, 10.0%; Br, 27.6% (O, 18.2%)]. FT-IR: ν (cm^{-1}) 3373 and 3182 [$NHC(NH_2)_2^+$], 2938 (CH), 1735 (C═O), 1657 (C═N).

Conjugation of Arg$_7$-Malt-NAcC$_{12}$ Acid to Fluorescein-Labeled Bovine Serum Albumin. Bovine serum albumin (BSA, 10 mg, 0.15 μmol) was dissolved in 250 μL of 0.1 M borate buffer, pH 8.3, and then added to 58 μL of a 10 mg/mL solution of FITC (0.15 μmol) in DMSO. The protein solution was left at room temperature under mild stirring for 1 h and then was added to 5.0 μL of ethanolamine (5 mg, 80 μmoles). The FITC-labeled protein (BSA-FITC) was purified by fast protein liquid chromatography (FPLC) using a Superose 12 gel-filtration column (Amersham-Pharmacia Biotech, Uppsala, Sweden) and was isocratically eluted with 0.5 mL/min of 100 mM phosphate buffer, pH 7.0. The fractions containing the fluorescent protein were pooled, lyophilized, and analyzed by

dx.doi.org/10.1021/bc200666u | Bioconjugate Chem. XXXX, XXX, XXX−XXX

Scheme 1. Synthesis of Oligo-Arginyl-*N*-Acetyl-Maltotriosylamido-Dodecanoic Acid (Arg_7-Malt-$NAcC_{12}$ acid)[a]

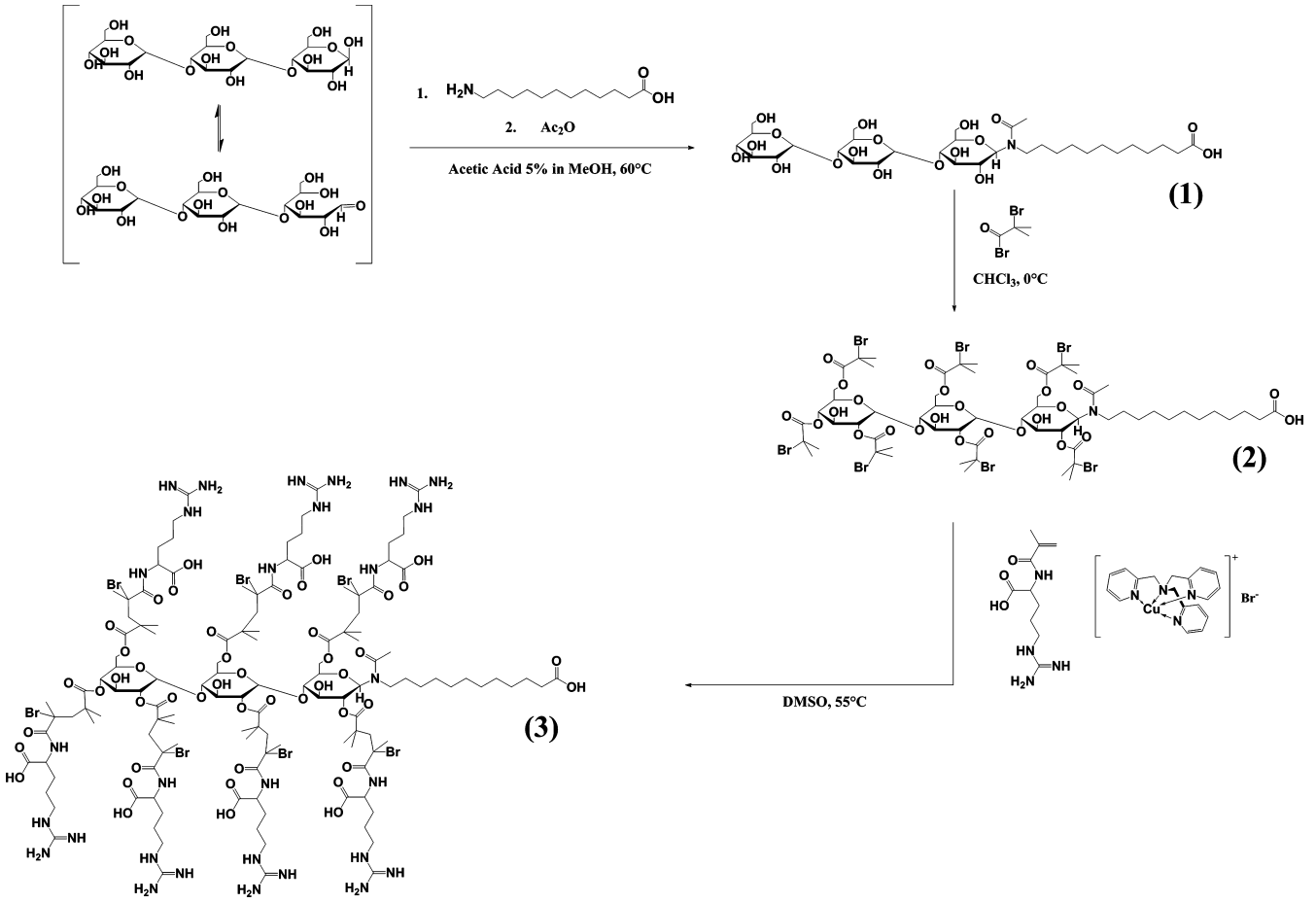

[a](1) Maltotriose derivatization with 12-amino-dodecanoic acid; (2) esterification of the maltotriosyl hydroxyl groups with 2-bromoisobutyryl bromide; (3) Arg-mathacryloylamide conjugation by ATRP reaction.

RP-HPLC using a Jupiter C4 column (250 × 4.6 mm, Phenomenex, Torrance, CA, USA) eluted with a gradient of H_2O/0.05% trifluoroacetic acid (A) and acetonitrile/0.05% trifluoroacetic acid (B) (0−3 min 5% B, 3−23 min from 5% to 55% B). The UV detector was set at 280 nm. The bioconjugation degree (number of FITC molecules per BSA molecule) was assessed by spectrophotometric determination of FITC at 494 nm ($Abs_{0.1\%\ p/v}$ = 184.9), and the protein was detected at 280 nm {$Abs_{0.1\%\ p/v}$ = 0.667; [BSA] = [$Abs_{280\ nm}$ − ($Abs_{494\ nm}$. 0.30)]/0.667}.

Following this, 100 μL of a solution of 5.5 mg/mL Arg_7-Malt-$NAcC_{12}$ acid (0.16 μmol) in DMSO was added to 1 mL of water containing 0.12 mg/mL EDC (0.63 μmol). After 30 min, the solution was added to 1.0 mL of 5.2 mg/mL FITC-BSA (0.08 μmol) in 0.1 M 2-(*N*-morpholino)ethane sulfonic acid, pH 4.6. The reaction mixture was stirred overnight and then ultrafiltered using an Amicon System equipped with a 10 kDa cutoff Ultrafree-CL membrane (Millipore Amicon, Bedford, MA, USA). The bioconjugate was finally purified by ion exchange chromatography using a TSK-GEL Chelate-5PW column eluted with a gradient of (A) 20 mM phosphate buffer, 0.1 M NaCl, pH 6.5; and (B) 20 mM phosphate buffer, 0.7 M NaCl, pH 6.5. The elution profile was analyzed online by UV at 280 nm and by fluorescence (λ_{ex} 494 nm; λ_{em} 520 nm). The peak detected by UV and fluorescence [(Arg_7-Malt-$NAcC_{12}$)$_2$-FITC-BSA] was collected, concentrated by ultrafiltration, and analyzed by RP-HPLC, as reported above. The number of Arg_7-Malt-$NAcC_{12}$ moieties per FITC-BSA molecule was determined by a Sakaguchi assay, using FITC-BSA as reference.

Cell Lines and Culture. The human MCF-7 breast adenocarcinoma and murine MC3T3-E1 embryonic fibroblast cell lines were grown in RPMI 1640 and DMEM medium, respectively, and supplemented with a mixture of 10% heat-inactivated fetal bovine serum (FBS), 1% L-glutamine, and a 1% penicillin−streptomycin−amphotericin B mixture. All cells were maintained at 37 °C in a humidified 5% CO_2 atmosphere and split every 2−3 days.

Cytotoxicity Assay. MCF-7 and MC3T3-E1 cells were plated in 96-well flat-bottomed microassay plates (1 × 10^4 cells/well) and grown for 24 h. After complete adhesion, Arg_7-Malt-$NAcC_{12}$ acid or polyethylenimine (PEI) was added to the culture media at increasing concentrations from 0 to 100 μM. The cells were incubated for 24 h at 37 °C, and then the medium was discarded by aspiration and replaced with 100 μL of fresh medium. The cells were grown for a further 48 h. Next, 20 μL of a 5 mg/mL solution of 3-(4,5-dimethylthiazol-2-yl)-2,5-diphenyltetrazolium bromide (MTT) in 20 mM phosphate buffer and 0.15 M NaCl, pH 7.2, was added to each well. After 4 h, the MTT-containing medium was removed and 200 μL of DMSO was added to each well to dissolve the formazan crystals formed by live cells.[36] The plates were gently shaken for 30 min and the absorbance was measured at 570 nm. The cell viability

dx.doi.org/10.1021/bc200666u | *Bioconjugate Chem.* XXXX, XXX, XXX−XXX

was expressed as a percent viability of treated cells with untreated cells used as a control.

Fluorescence Analysis. MCF-7 and MC3T3-E1 cells were seeded in 12-well plates (5×10^5 cells/well). After 48 h (90% confluence), the medium was removed and the cells were incubated with FITC-BSA or $(Arg_7\text{-Malt-NAcC}_{12})_2$-FITC-BSA (0.2 μM in culture medium supplemented with 10% FBS) at 37 or 4 °C. After 60 min, the medium was removed and the cells were washed three times with DPBS and lysed in 1 mL of 0.1% Triton X-100 solution. The plates were gently shaken for 2 h and the lysates were centrifuged at 12 000 rpm (10 625 g) for 5 min. The fluorescence intensity was measured at 520 nm by a FP-6500 Jasco Fluorescence Spectrophotometer (Kyoto, Japan) using 0.1% Triton X-100 as the blank. A similar procedure was carried out with unseeded plates to quantify the fluorescence intensity of the background. The relative fluorescence (fluorescence/cell number) was calculated by determining the cell number on the basis of the BCA protein assay (Pierce, Celbio, Pero, Italy). The optical density (O.D.) data at 570 nm were plotted on a standard curve (O.D. values vs cells/mL; $y = 10^{-6}\,x + 0.024$, $R^2 = 0.996$).

Fluorescence-Activated Cell Sorting (FACS) Analysis. MCF-7 and MC3T3-E1 cells were seeded in six-well plates (1×10^6 cells/well, 1.8 mL culture medium/well). After 48 h, the medium was removed and the cells were washed with 1.8 mL of DPBS and incubated with FITC-BSA or $(Arg_7\text{-Malt-NAcC}_{12})_2$-FITC-BSA (0.2 μM in culture medium supplied with 10% FBS), as described above. After 60 min of incubation at 37 °C, the cells were washed three times with DPBS and treated for 2 min with trypsin/EDTA. Trypsin-treated cells were recovered by centrifugation at 1500 rpm (166 g) for 2 min and were washed twice with DPBS. The cells were fixed with 1% (w/v) paraformaldehyde in phosphate buffer and stored overnight at 4 °C, protected from light. Afterward, the cell samples (100 000 cells in average count) were analyzed by a FACSCalibur flow cytometer using the *CellQuest* software package (BD Bioscience, Heidelberg, Germany) and then gated using forward vs side scatter to exclude debris and dead cells.

Confocal Microscopy. MCF-7 and MC3T3-E1 cells were plated on four-well chamber slides at a density of 1×10^5 cells per chamber and incubated at 37 °C in a humidified 5% CO_2 atmosphere. After 24 h of adhesion, the cells were incubated with FITC-BSA or $(Arg_7\text{-Malt-NAcC}_{12})_2$-FITC-BSA (0.2 μM in culture medium supplemented with 10% FBS), as described above. After 60 min incubation at 37 °C, the cells were thoroughly washed with DPBS and fixed with 1% (w/v) paraformaldehyde in phosphate buffer for 1 h at 4 °C. Afterward, the fixed cells were rinsed twice with DPBS, and the samples were mounted with Vectashield containing 1.5 μg/mL DAPI and kept at 4 °C. The cells were protected from light until microscopic examination. Confocal imaging was performed using a Leica TCS SP5 confocal laser-scanning microscope (Leica Microsystems, Mannheim, Germany) equipped with a Leica HCX PL APO 63×/1.40 oil immersion objective. The blue argon laser was set at 351 nm (blue) and 488 nm[9] to produce the excitation wavelengths for DAPI and fluorescein, respectively.

RESULTS

Synthesis and Characterization of Hepta-Arginyl-*N*-Acetyl-Maltotriosylamido-Dodecanoic Acid (Arg_7-Malt-$NAcC_{12}$ acid). The synthesis of hepta-arginyl-*N*-acetyl-maltotriosylamido-dodecanoic acid (Arg_7-Malt-$NAcC_{12}$ acid) was carried out according to a three-step procedure described in Scheme 1: (1) synthesis of maltotriosylamido-dodecanoic acid (Malt-C_{12} acid) and *N*-acetylation of the amino group of Malt-C_{12} acid (Malt-$NAcC_{12}$ acid); (2) synthesis of hepta-(2-bromoisobutyryl)-*N*-acetyl-maltotriosylamido-dodecanoic acid ($BrIsoBut_7$-Malt-$NAcC_{12}$ acid); (3) synthesis of hepta-arginyl-*N*-acetyl-maltotriosylamido-dodecanoic acid (Arg_7-Malt-$NAcC_{12}$ acid).

The synthesis of Malt-C_{12} acid was carried out through the reaction of the amino group of 12-amino-dodecanoic acid with the reducible anomeric carbon of maltotriose. The resulting amino group was stabilized by acetylation at the nitrogen to avoid the detachment of the 12-amino-dodecanoic acid residue. The synthesis and purification process yielded an approximate 70% molar yield (Malt-C_{12} acid/maltotriose, mol/mol %). The HPLC analysis of Malt-C_{12} acid showed a single sharp peak, which indicated that the product was pure. The chemical composition of the conjugate was confirmed by elemental analysis, FT-IR, ^{1}H NMR, and ESI-MS (see Materials and Methods). FT-IR showed the presence of characteristic signals corresponding to the hydroxyl groups of the maltotriosyl residue, C−H bonds and the terminal carboxyl group of the alkyl moiety and the acetyl functionality. The ^{1}H NMR showed the presence of typical signals of Malt-$NAcC_{12}$ acid. Mass spectrometry analysis showed the correspondence of the final product mass with the expected value. These results confirmed the chemical identity of the monoacetylated conjugate.

The carbohydrate hydroxyl groups of Malt-$NAcC_{12}$ acid were esterified with 2-bromo-isobutyryl bromide to obtain a multiarmed oligosaccharide initiator for ATRP reaction. The FT-IR analysis showed the nearly complete disappearance of the glycosidic OH signal at 3437 cm^{-1}, which indicates the extensive functionalization of the hydroxyl groups with 2-bromo-isobutyryl bromide. The intensity of the signals of the acetyl and alkyl terminating carbonyl groups at 1741 and 1619 cm^{-1} were unaffected by the conjugation reaction. The ^{1}H NMR showed the presence of the typical signals corresponding to the oligo-2-bromoisobutyryl derivative (see Materials and Methods). The elemental analysis showed that the composition of the multiarmed initiator corresponded to $BrIsoBut_7$-Malt-$NAcC_{12}$ acid indicating that 7 out of the 10 available hydroxyl groups were modified with 2-bromo-isobutyryl-bromide. On the basis of these data, the calculated molecular weight of the novel bioconjugate was 3482 Da. The synthesis of $BrIsoBut_7$-Malt-$NAcC_{12}$ acid resulted in approximately 60% product yield [$BrIsoBut_7$-Malt-$NAcC_{12}$ acid/Malt-$NAcC_{12}$ acid, mol/mol %].

The conjugation of the arginyl residues to the $BrIsoBut_7$-Malt-$NAcC_{12}$ acid was carried out under ATRP conditions using arginine-methacryloylamide (Arg-methacryloylamide) as the monomer and tris[(2-pyridyl)methyl]amine (TPMA) as the ligand for $Cu(I)^+$. Both Arg-methacryloylamide and TPMA were prepared with high product yields, 99% and 64%, respectively, and in high purity.

The reaction was carried out under an atmosphere of nitrogen to avoid the catalyst inactivation by oxidation of Cu(I) to Cu(II). The reaction also used a 2:1 molar excess of Arg-methacryloylamide with respect to the 2-bromo-isobutyryl residues to obtain complete 2-bromo-isobutyryl derivatization. The ^{1}H NMR spectrum of the purified final product (Figure 1A) was complex, but did show the presence of the triplet at 3.35 ppm (J = 6.8 Hz) corresponding to the δ-CH_2 of arginyl moieties. The two singlets at 5.69 and 5.47 ppm, corresponding to the methacrylic functionality, were also absent, confirming

dx.doi.org/10.1021/bc200666u | *Bioconjugate Chem.* XXXX, XXX, XXX–XXX

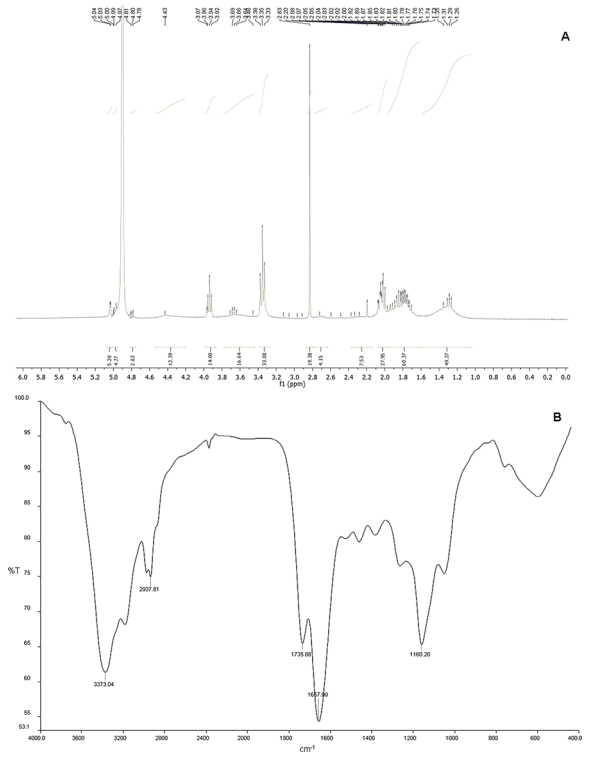

Figure 1. ^{1}H NMR spectrum (A) and IR spectrum (B) of hepta-arginyl-*N*-acetyl-maltotriosylamido-undecanoyl acid (Arg_7-Malt-$NAcC_{12}$ acid).

the absence of unreacted monomer. The IR spectrum (Figure 1B) confirmed the presence of the guanidine functions. These data indicated the conjugation of the Arg-methacryloylamide to the oligosaccharide structure, and elemental analysis suggested the hepta-arginyl derivative. This result was confirmed by the colorimetric determination of the arginyl groups by the Sakaguchi assay.

Cytotoxicity Assay. The cytotoxicity of Arg_7-Malt-$NAcC_{12}$ acid was investigated by incubation for 24 h in the presence of MCF-7 and MC3T3-E1 cells. A comparative cell viability assay was carried out using polyethylenimine (PEI) with a similar average molecular weight of Arg_7-Malt-$NAcC_{12}$ acid.

The cytotoxicity profiles reported in Figure 2 show that the Arg_7-Malt-$NAcC_{12}$ acid has a very low toxicity toward both of the examined cell lines compared to PEI. The IC_{50} measured for PEI was 40 and 30 μM for MCF-7 and MC3T3-E1, respectively, while for the Arg_7-Malt-$NAcC_{12}$ acid, the obtained IC_{50} with both cell lines was higher than 100 μM.

Preparation of Hepta-Arginyl-*N*-Acetyl-Maltotriosylamido-Dodecanoyl-FITC-BSA [$(Arg_7$-Malt-$NAcC_{12})_2$-FITC-BSA]. Bovine serum albumin (BSA, 66 kDa, isoelectric point 4.7) was used as a cargo model to assess the ability of Arg_7-Malt-$NAcC_{12}$ acid to act as an intracellular carrier for hydrophilic macromolecules.

The conjugation of Arg_7-Malt-$NAcC_{12}$ acid to fluorescein-labeled BSA (FITC-BSA) (Scheme 2) was carried out by EDC-mediated condensation. The chromatographic and spectroscopic analyses of the purified product showed the conjugation of FITC-BSA to Arg_7-Malt-$NAcC_{12}$ acid. The Sakaguchi assay showed that the Arg_7-Malt-$NAcC_{12}$ acid-derivatized FITC-BSA contained a mean of two Arg_7-Malt-$NAcC_{12}$ moieties per FITC-BSA molecule, yielding $(Arg_7$-Malt-$NAcC_{12})_2$-FITC-BSA.

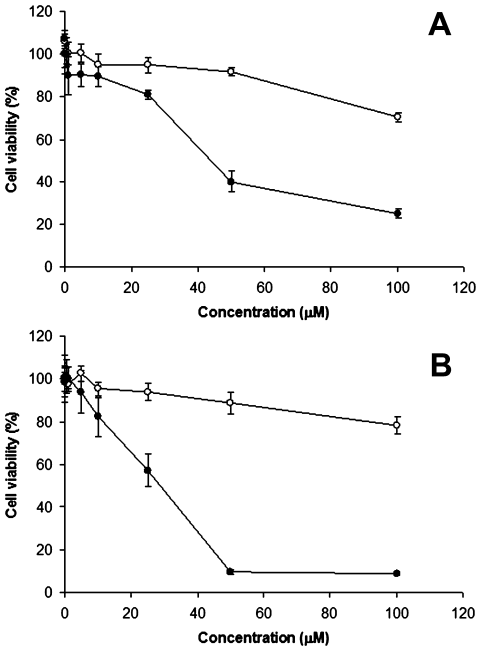

Figure 2. Cytotoxicity profiles obtained by MCF-7 (A) and MC3T3-E1 (B) incubation with increasing concentrations of polyethylenimine (●) and hepta-arginyl-*N*-acetyl-maltotriosylamido-dodecanoic acid (○). The mean values and standard deviations were calculated on the basis of values obtained from six experiments.

Fluorimetric Assays. *In vitro* studies were undertaken to evaluate the ability of Arg_7-Malt-$NAcC_{12}$ acid to transport hydrophilic macromolecules into cells. MCF-7 and MC3T3-E1 cells were incubated with FITC-BSA or $(Arg_7$-Malt-$NAcC_{12})_2$-FITC-BSA, and the protein uptake was evaluated by spectrofluorimetric analysis, flow cytometry, and confocal microscopy.

Since studies reported in the literature showed that tumor cells, namely, MCF-7 cells, can internalize serum proteins including serm albumin,[37,38] FITC-BSA was used as control.

Before the fluorimetric analyses, the cells were extensively washed with buffer to eliminate the FITC-BSA or $(Arg_7$-Malt-$NAcC_{12})_2$-FITC-BSA that was not taken up by the cells.

Spectrofluorimetric Analysis. The cell-associated relative fluorescence (RF) was examined after MCF-7 and MC3T3-E1 incubation at 37 and 4 °C with FITC-BSA and $(Arg_7$-Malt-$NAcC_{12})_2$-FITC-BSA and cell lysis with Triton X/100. To compare the results obtained under different conditions, the relative fluorescence (RI) values were normalized to 10^6 cells.

Figure 3 reports the RF obtained by cell incubation at 37 °C with buffer (self-fluorescence), FITC-BSA, and $(Arg_7$-Malt-$NAcC_{12})_2$-FITC-BSA. The RF associated with the MCF-7 and MC3T3-E1 cells incubated with FITC-BSA was in agreement with the evidence reported in the literature that serum albumin can be taken up by tumor cells.[37,38] The fluorescence intensity values obtained by MCF-7 and MC3T3-E1 cell incubation with $(Arg_7$-Malt-$NAcC_{12})_2$-FITC-BSA were approximately 4.5 times higher than those obtained with FITC-BSA-treated cells.

Figure 4 shows the RF values obtained by MCF-7 and MC3T3-E1 incubation with buffer, FITC-BSA, and $(Arg_7$-Malt-$NAcC_{12})_2$-FITC-BSA at 4 °C. The basal cell RF of untreated MCF-7 and MC3T3-E1 cells was similar to that obtained at 37°, while the RF obtained with FITC-BSA and $(Arg_7$-Malt-$NAcC_{12})_2$-FITC-BSA was significantly lower. The incubation with FITC-BSA resulted in an approximate 2-fold RF increase

dx.doi.org/10.1021/bc200666u | *Bioconjugate Chem.* XXXX, XXX, XXX–XXX

Scheme 2. Synthesis of Fluorescent Hepta-Arginyl-*N*-Acetyl-Maltotriosylamido-Undecanoyl-BSA [$(Arg_7$-Malt-$NAcC_{12})_2$-FITC-BSA]

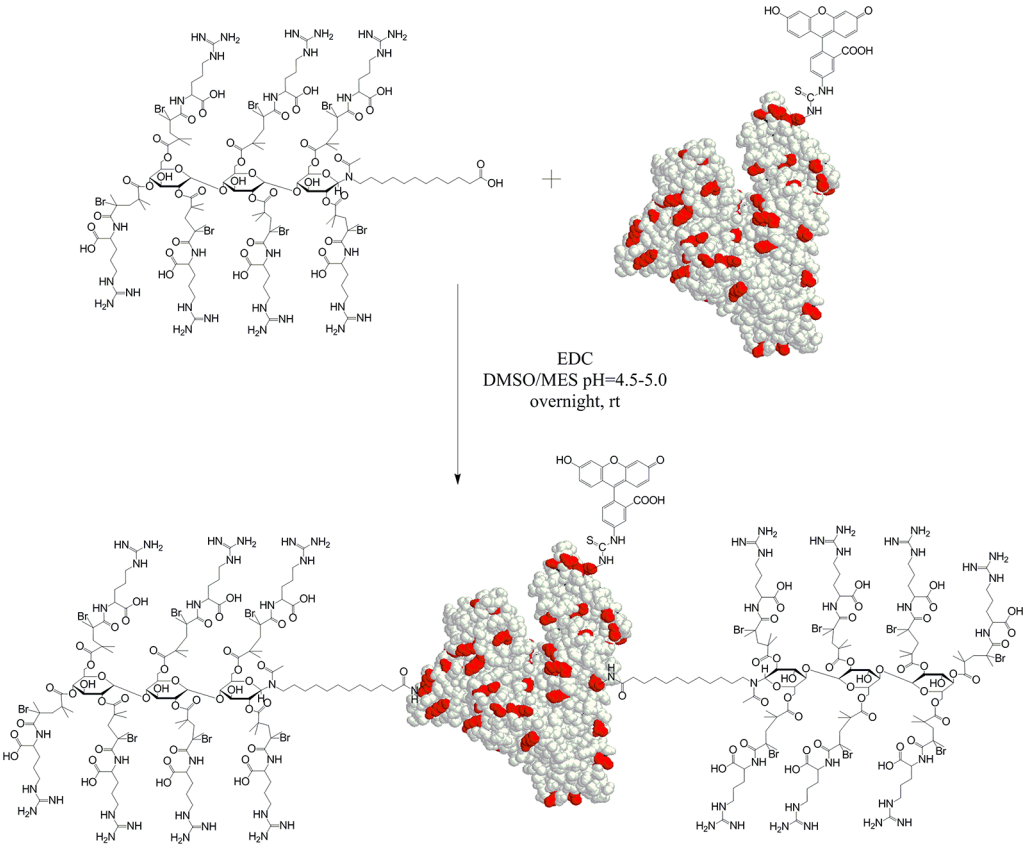

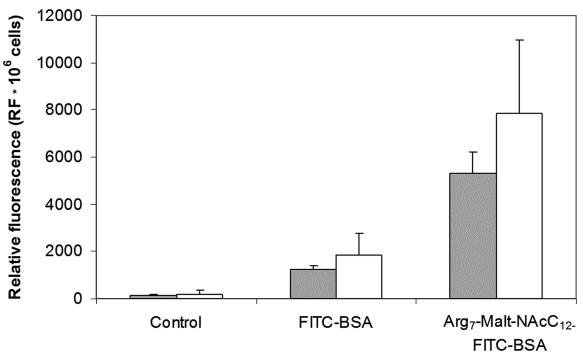

Figure 3. Relative fluorescence of lysated MCF-7 cells (white) and MC3T3-E1 cells (gray) incubated at 37 °C with buffer (control), FITC-BSA, and hepta-arginyl-N-acetyl-maltotriosylamido-dodecanoyl-FITC-BSA. The mean values and standard deviations were calculated on the basis of values obtained from five experiments.

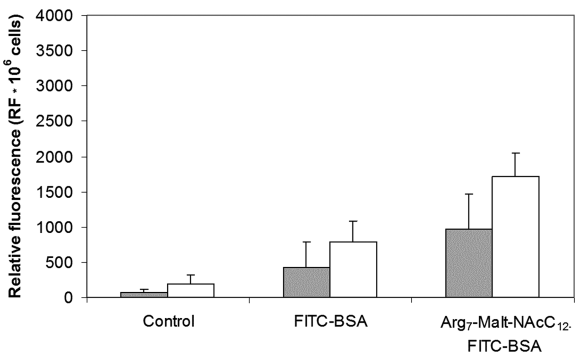

Figure 4. Relative fluorescence of lysated MCF-7 cells (white) and MC3T3-E1 cells (gray) incubated at 4 °C with buffer (control), FITC-BSA, and hepta-arginyl-N-acetyl-maltotriosylamido-dodecanoyl-FITC-BSA. The mean values and standard deviations were calculated on the basis of values obtained from five experiments.

compared to the basal cell RF, and the RF of MCF-7 and MC3T3-E1 cells incubated with $(Arg_7$-Malt-$NAcC_{12})_2$-FITC-BSA was 2 times higher than that obtained with the cells incubated with FITC-BSA.

Flow Cytometry Analysis. Figure 5 reports the dot plots of side scatter (SSC-H) vs fluorescence intensity (FL1-H) obtained by fluorescence-activated cell sorting. The plots reported in panels A2 and B2 show that the percentage of FITC-BSA-treated MCF-7 and MC3T3-E1 cells with higher fluorescence were lower than 8% and 11%, respectively, compared to the untreated cells (panels A1 and B1). The dot plots reported in panels A3 and B3 show that the incubation with $(Arg_7$-Malt-$NAcC_{12})_2$-FITC-BSA significantly increases the cell-associated fluorescence. Over 85% and 95% of the $(Arg_7$-Malt-$NAcC_{12})_2$-FITC-BSA treated MCF-7 and MC3T3-E1 cells, respectively, displayed higher fluorescence compared to the self-fluorescence of untreated cells.

Confocal Microscopy. The confocal images obtained with MCF-7 and MC3T3-E1 cells incubated with FITC-BSA and $(Arg_7$-Malt-$NAcC_{12})_2$-FITC-BSA are reported in Figures 6 and 7, respectively. Figures 6A and 7A report the images obtained after 60 min cell incubation at 37 °C, while Figures 6B and 7B report the images obtained after cell incubation at 4 °C. In order to evidence the fluorescence of $(Arg_7$-Malt-$NAcC_{12})_2$-

dx.doi.org/10.1021/bc200666u | *Bioconjugate Chem.* XXXX, XXX, XXX–XXX

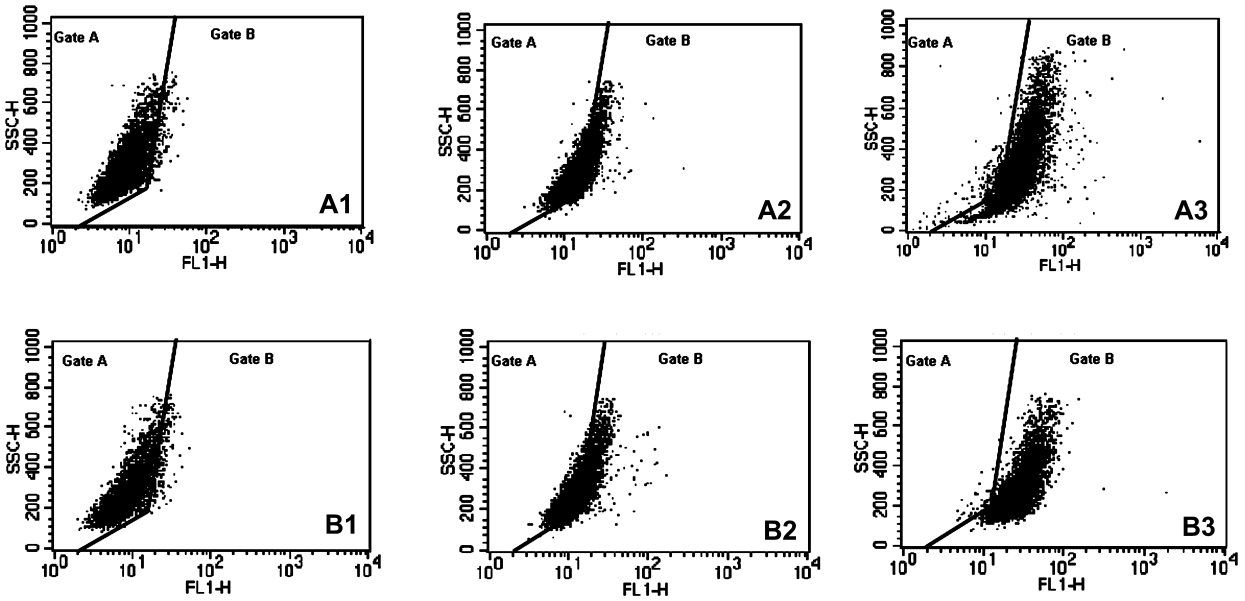

Figure 5. Side scatter (SSC-H) versus fluorescence (FL1-H) plots obtained by flow-activated cytometry sorting analysis of MCF-7 (A) and MC3T3-E1 (B) cells after incubation with plain buffer (A1 and B1), FITC-BSA (A2 and B2), and hepta-arginyl-*N*-acetyl-maltotriosylamido-dodecanoyl-FITC-BSA (A3 and B3).

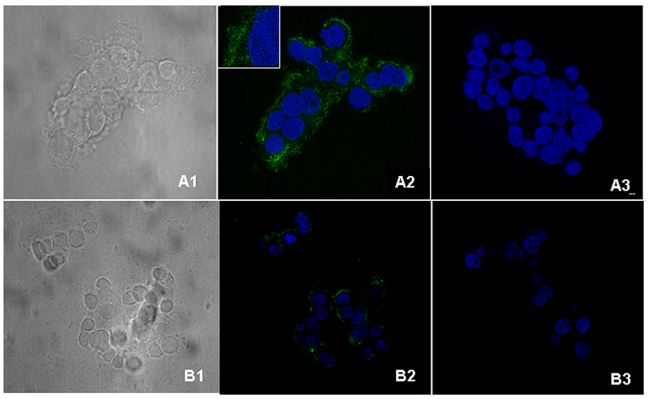

Figure 6. Confocal microscopy images (63×) obtained with MCF-7 incubated for 60 min with (A) $(Arg_7\text{-Malt-NAcC}_{12})_2$-FITC-BSA at 37 °C (A1, transmission image; A2, reflection image) and FITC-BSA (A3); (B) $(Arg_7\text{-Malt-NAcC}_{12})_2$-FITC-BSA at 4 °C (B1, transmission image; B2, reflection image) and FITC-BSA (B3). The green fluorescence obtained with FITC-BSA was set as basal level.

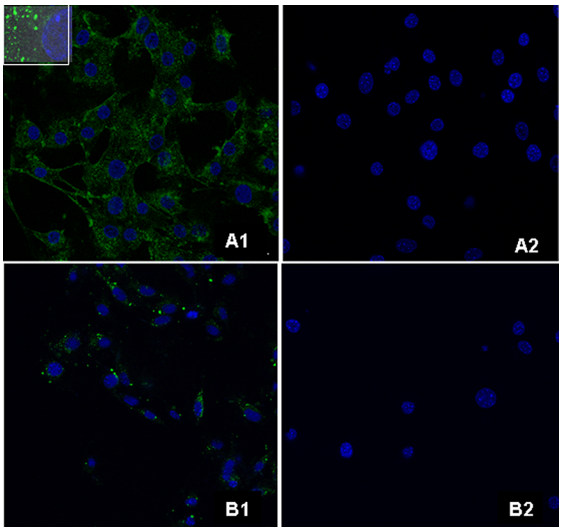

Figure 7. Confocal microscopy images (63×) obtained with MC3T3-E1 incubated for 60 min with (A) $(Arg_7\text{-Malt-NAcC}_{12})_2$-FITC-BSA at 37 °C (A1) and FITC-BSA (A3); (B) $(Arg_7\text{-Malt-NAcC}_{12})_2$-FITC-BSA at 4 °C (B1) and FITC-BSA (B3). The green fluorescence obtained with FITC-BSA was set as basal level.

FITC-BSA internalized by the cells. the fluorescence of FITC-BSA treated MCF-7 (Figure 6A3,B3) and MC3T3-E1 cells (and Figure 7A2,B2) has been set as basal level. Therefore, the images obtained with the control cells (Figures 6A3,B3 and 7A2,B2) show the intense blue fluorescence corresponding to DAPI-stained nuclei only. The images obtained with $(Arg_7\text{-Malt-NAcC}_{12})_2$-FITC-BSA-treated MCF-7 (Figure 6A2,B2) and MC3T3-E1 cells (Figure 7A1,B1) show intense green fluorescence in the cytosol. The inset of Figures 6A2 and 7A1 show the punctuated fluorescence distribution in the cytosol. The images obtained with cells incubated at 4 °C (Figures 6B and 7B) show that $(Arg_7\text{-Malt-NAcC}_{12})_2$-FITC-BSA is taken up by the cells at a lower extent. This qualitative result confirms the data obtained by spectrofluorimetry and FACS. Finally, green fluorescence was never found in the nuclei.

DISCUSSION

The nonlinear oligo-arginyl cell-penetrating enhancer Arg_7-Malt-$NAcC_{12}$ acid was designed for conjugation to large systems, namely, proteins, oligonucleotides, or colloidal drug carriers, to promote their cell entry. The nonconventional architecture of this bioconjugate was obtained by introducing arginyl moieties, which are the key functions of the cell-penetrating 49−57 Tat, to a core anchoring structure. The synthesis protocol was originally designed to obtain a series of derivatives with a nonpeptidic structure containing a variable number of Arg functions attached to an anchoring structure that could perform as a cell-penetration enhancer.

Maltotriose was selected as the anchoring molecule. The hydroxyl groups of this molecule can provide for multiple

dx.doi.org/10.1021/bc200666u | *Bioconjugate Chem.* XXXX, XXX, XXX−XXX

derivatizations with arginyl residues through simple chemical protocols to obtain a nonpeptide, star-like construct. In addition, the peculiar reactivity of the reducible anomeric carbon of maltotriose toward amines can be exploited to introduce functional groups, namely, −COOH, $-NH_2$, −SH, and so forth, for conjugation to macromolecules or supramolecular drug delivery systems.

According to the chemical features of maltotriose, the anomeric carbon of the oligosaccharide was functionalized with linear alkyl chains of 12-amino-dodecanoic acid, and the resulting amino group was stabilized by N-acetylation. Spectrophotometric and elemental analysis showed that the acetylation reaction involved only the amino group of the conjugate, while the hydroxyl functions of maltotriose were not acetylated and remained available for the following modification steps.

The conjugation of arginine functions to Malt-$NAcC_{12}$ acid was carried out under ATRP conditions, a technique that yields macromolecular products with defined composition under controlled reaction conditions.[39,40] Accordingly, Malt-$NAcC_{12}$ acid was first converted into a multiarmed initiator by reaction with 2-bromo-isobutyryl bromide. The acid was then reacted in the presence of Arg-methacryloylamide, using TPMA/Cu(I)Br as the catalytic system.

The incomplete maltotriose hydroxyl substitution with 2-bromo-isobutyryl bromide (7 out of the 10 available OH) that occurred despite the use of excess 2-bromo-isobutyryl bromide/Malt-$NAcC_{12}$ acid molar ratios may be ascribed to steric hindrance that prevents the 2-bromo-isobutyryl-bromide from reacting with the two vicinal hydroxyl groups of the oligosaccharide.

Under ATRP conditions, 7 Arg-methacryloylamido moieties were attached to the $BrIsoBut_7$-Malt-$NAcC_{12}$. Preliminary studies showed that the derivatization of maltotriose bearing two and four 2-bromo-isobutyryl functions resulted in the maximal conjugation of two and four Arg-methacryolylamido moieties, respectively (data not shown). These results seem to suggest that, under the operative conditions, the 2-bromo-isobutyryl-bromide groups are completely functionalized with one Arg-methacryloylamido moiety. Indeed, even the use of high molar ratios of Arg-methacryloylamide/$BrIsoBut_7$-Malt-$NAcC_{12}$ (14:1 and 21:1) did not yield higher Arg-methacryloylamido functionalization. Therefore, for bioconjugates bearing short Arg-methacryloylamido chains, the Arg-methacryloylamide oligomerization could not be obtained. In this regard, studies reported in the literature have demonstrated that the inefficient polymerization of (meth)acrylamide monomers may be ascribed to various phenomena, including catalyst deactivation by the amido groups and the strong bond between the (meth)acrylamide units and the bromide atom.[41,42]

The bioconjugate containing 7 Arg residues that is described in the present study displays composition analogies with cell-penetration peptides, such as the 49−57 Tat domain and oligoarginine peptides. Therefore, it was considered a good candidate as a penetration enhancer for further biological investigations.

Cell culture studies showed that the novel nonlinear hepta-arginyl derivative does not exhibit significant cytotoxicity, which is a requisite for a new product that is expected to undergo intracellular localization. The high IC_{50} (>100 μM) and the fact that only a limited amount of enhancer may be required for promoting the cell translocation of colloidal formulations suggest that this product is potentially safe for pharmaceutical applications. However, since the nonlinear hepta-arginyl derivative has been designed for conjugation to macromolecules or supramolecular drug vehicles, the short- and long-term toxicity of each colloidal bioconjugate containing the star-like oligo-arginyl-maltotriosyl derivative must be investigated in detail.

The most common way to confirm the cell-penetrating efficiency of different CPPs has been through labeling with fluorophores, such as fluorescein or rhodamine. Therefore, the cell-penetrating properties of the Arg_7-Malt-$NAcC_{12}$ derivative were evaluated using BSA as a cargo molecule labeled with fluorescein isothiocyanate (FITC).

The spectrofluorimetric analyses, fluorescence activated cell sorting, and confocal microscopy showed that, as with other Arg rich macromolecules described in the literature,[43] Arg_7-Malt-$NAcC_{12}$ can bestow promising cell-penetration properties on macromolecular bioconjugates.

The quantitative fluorescence studies and the cytofluorimetric analyses showed that both the MC3T3-E1 and the MCF-7 cell lines underwent (Arg_7-Malt-$NAcC_{12}$)$_2$-FITC-BSA uptake. The slight differences observed between the MC3T3-E1 and the MCF-7 cells appear to indicate that the translocation process may depend on surface cell-specific properties, such as specific membrane biological activity or membrane composition.

Confocal microscopy confirmed the cell uptake of (Arg_7-Malt-$NAcC_{12}$)$_2$-FITC-BSA. The punctuated fluorescence distribution in the cytosol obtained with the cells treated with (Arg_7-Malt-$NAcC_{12}$)$_2$-FITC-BSA and the lack of fluorescence in the nucleus indicate that the cell uptake of (Arg_7-Malt-$NAcC_{12}$)$_2$-FITC-BSA was limited to the cytoplasm compartment. This result is in agreement with the data reported in the literature, which showed that branching membrane translocational peptides promote gene delivery in the cytoplasm, but not in the nucleus.[44]

The cell trafficking of arginine-rich CPPs is still controversial. The cell uptake of cargo-CCPs has been found to occur according to mechanisms and kinetics that depend on the chemical nature of the cell-penetrating function and assay conditions, namely, temperature, pH, cargo-CCP dose, and so forth.[45] The arginine-rich CPPs were found to destabilize the plasma membrane, creating transient pores for cellular penetration that resulted in cytosol or nucleus localization without organelle confinement. Nevertheless, the confocal results obtained with the cells incubated with (Arg_7-Malt-$NAcC_{12}$)$_2$-FITC-BSA indicate that active mechanisms may be involved in or contribute to the cell uptake of the bioconjugate. The punctuated fluorescence obtained by the confocal analysis of cells incubated with (Arg_7-Malt-$NAcC_{12}$)$_2$-FITC-BSA at 37 °C seems, in fact, to corroborate the hypothesis that the star-like penetration enhancer promotes the macromolecular cargo uptake by endocytosis or macropinocytosis.[46] This hypothesis is also confirmed by the data obtained at 4 °C. Under these conditions, the active cell uptake is minimized and the cell translocation of (Arg_7-Malt-$NAcC_{12}$)$_2$-FITC-BSA was significantly lower than that obtained at 37 °C. However, the lower FITC-BSA uptake observed at 4 °C compared to that obtained at 37 °C may be ascribed to the temperature-related permeability impairment of the cell membrane. Therefore, the lower cell uptake of (Arg_7-Malt-$NAcC_{12}$)$_2$-FITC-BSA at 4 °C could be related to both the inhibition of the active

dx.doi.org/10.1021/bc200666u | Bioconjugate Chem. XXXX, XXX, XXX−XXX

translocation and the lower passive diffusion due to decreased membrane permeability.

The combined biological data emphasize the complexity of the cell uptake process that is mediated by the novel penetrating agent. Currently, studies have been undertaken to elucidate the cellular mechanisms involved in the translocation of Arg_7-Malt-$NAcC_{12}$ functions. These studies are aimed at comparatively examining the cell-penetrating properties of the corona-like derivative and linear TAT-like sequences. Additional investigations will also be performed using different cell lines and experimental conditions, namely, time, pH, and temperature.

CONCLUSIONS

The results reported in the present work show that a novel class of cell-penetration enhancers with unusual chemical structures can be easily obtained via simple and reproducible synthetic steps. In principle, the proposed chemical synthesis protocol is flexible and can be properly managed to obtain products that, by virtue of their unconventional structural properties, open new possibilities in drug delivery.

A wide array of cell-penetration enhancers can be obtained by slight modifications of the main structure of these enhancers to provide for their conjugation or physical combination with a variety of therapeutic systems. These molecules can be designed for conjugation to proteins or polymer therapeutics, or for surface decoration of liposomes or nanoparticles. The cationic features and the penetration-enhancing properties of the star-like oligo-arginyl can also be exploited for oligonucleotide, namely, siRNA, or gene delivery.

Finally, a combination of residues, such as histidines and cysteines, that have been found to possess endosomolytic properties or short peptides that increase the gene expression of DNAs, can be introduced within the core structure.

AUTHOR INFORMATION

Corresponding Author

*E-mail: paolo.caliceti@unipd.it; phone +39 049 8275695; fax +39 049 8275366.

Notes

The authors declare no competing financial interest.

REFERENCES

(1) Amidon, G. L., Lennernäs, H., Shah, V. P., and Crison, J. R. (1995) A theoretical basis for a biopharmaceutic drug classification: the correlation of in vitro drug product dissolution and in vivo bioavailability. *Pharm. Res. 12*, 413−420.

(2) Williams, A. C., and Barry, B. W. (2004) Penetration enhancers. *Adv. Drug Delivery Rev. 56*, 603−618.

(3) Wadia, J. S., and Dowdy, S. F. (2002) Protein transduction technology. *Curr. Opin. Biotechnol. 13*, 52−56.

(4) Stewart, K. M., Horton, K. L., and Kelley, S. O. (2008) Cell-penetrating peptides as delivery vehicles for biology and medicine. *Org. Biomol. Chem. 6*, 2242−2255.

(5) Fonseca, S. B., Pereira, M. P., and Kelley, S. O. (2009) Recent advances in the use of cell-penetrating peptides for medical and biological applications. *Adv. Drug Delivery Rev. 61*, 953−964.

(6) Tung, C.-H., and Weissleder, R. (2003) Arginine containing peptides as delivery vectors. *Adv. Drug Delivery Rev. 55*, 281−294.

(7) Jeyapaul, J., Reddy, M. R., and Khan, S. A. (1990) Activity of synthetic tat peptides in human immunodeficiency virus type 1 long terminal repeat-promoted transcription in a cell-free system. *Proc. Natl. Acad. Sci. U.S.A. 87*, 7030−4.

(8) Kalderon, D., Roberts, B. L., Richardson, W. D., and Smith, A. E. (1984) A short amino acid sequence able to specify nuclear location. *Cell 39*, 499−509.

(9) Green, M., and Loewenstein, P. M. (1988) Autonomous functional domains of chemically synthesized human immunodeficiency virus tat trans-activator protein. *Cell 55*, 1179−1188.

(10) Futaki, S., Suzuki, T., Ohashi, W., Yagami, T., Tanaka, S., Ueda, K., and Sugiura, Y. (2001) Arginine-rich Peptides. *J. Biol. Chem. 276*, 5836−5840.

(11) Futaki, S. (2006) Oligoarginine vectors for intracellular delivery: Design and cellular-uptake mechanisms. *Pept. Sci. 84*, 241−249.

(12) Patel, L., Zaro, J., and Shen, W.-C. (2007) Cell penetrating peptides: intracellular pathways and pharmaceutical perspectives. *Pharm. Res. 24*, 1977−1992.

(13) Wagstaff, K. M., and Jans, D. A. (2006) Protein transduction: cell penetrating peptides and their therapeutic applications. *Curr. Med. Chem. 13*, 1371−87.

(14) Okuyama, M., Laman, H., Kingsbury, S. R., Visintin, C., Leo, E., Eward, K. L., Stoeber, K., Boshoff, C., Williams, G. H., and Selwood, D. L. (2007) Small-molecule mimics of an [alpha]-helix for efficient transport of proteins into cells. *Nat. Meth. 4*, 153−159.

(15) Fisher, A. A., Ye, D., Sergueev, D. S., Fisher, M. H., Shaw, B. R., and Juliano, R. L. (2002) Evaluating the specificity of antisense oligonucleotide conjugates. *J. Biol. Chem. 277*, 22980−22984.

(16) Veldhoen, S., Laufer, S., and Restle, T. (2008) Recent developments in peptide-based nucleic acid delivery. *Int. J. Mol. Sci. 9*, 1276−1320.

(17) Dostmann, W. R. G., Taylor, M. S., Nickl, C. K., Brayden, J. E., Frank, R., and Tegge, W. J. (2000) Highly specific, membrane-permeant peptide blockers of cgmp-dependent protein kinase iα inhibit no-induced cerebral dilation. *Proc. Natl. Acad. Sci. U.S.A. 97*, 14772−14777.

(18) Bonny, C., Oberson, A., Negri, S., Sauser, C., and Schorderet, D. F. (2001) Cell-permeable peptide inhibitors of JNK. *Diabetes 50*, 77−82.

(19) Patsch, C., and Edenhofer, F. (2007) , *Conditional Mutagenesis by Cell-Permeable Proteins: Potential Limitations and Prospects Conditional Mutagenesis: An Approach to Disease Models* (Feil, R., and Metzger, D., Eds.) pp 203−232, Springer, Berlin.

(20) Säälik, P., Elmquist, A., Hansen, M., Padari, K., Saar, K., Viht, K., Langel, Ü., and Pooga, M. (2004) Protein cargo delivery properties of cell-penetrating peptides. a comparative study. *Bioconjugate Chem. 15*, 1246−1253.

(21) Albarran, B., To, R., and Stayton, P. S. (2005) A TAT−streptavidin fusion protein directs uptake of biotinylated cargo into mammalian cells. *Protein Eng., Des. Sel. 18*, 147−152.

(22) Torchilin, V. P. (2008) Tat peptide-mediated intracellular delivery of pharmaceutical nanocarriers. *Adv. Drug Delivery Rev. 60*, 548−558.

(23) Medintz, I. L., Pons, T., Delehanty, J. B., Susumu, K., Brunel, F. M., Dawson, P. E., and Mattoussi, H. (2008) Intracellular delivery of quantum dot−protein cargos mediated by cell penetrating peptides. *Bioconjugate Chem. 19*, 1785−1795.

(24) Liu, B. R., Huang, Y.-w., Winiarz, J. G., Chiang, H.-J., and Lee, H.-J. (2011) Intracellular delivery of quantum dots mediated by a histidine- and arginine-rich HR9 cell-penetrating peptide through the direct membrane translocation mechanism. *Biomaterials 32*, 3520−3537.

(25) Tréhin, R., and Merkle, H. P. (2004) Chances and pitfalls of cell penetrating peptides for cellular drug delivery. *Eur. J. Pharm. Biopharm. 58*, 209−223.

(26) Sakuma, S., Suita, M., Masaoka, Y., Kataoka, M., Nakajima, N., Shinkai, N., Yamauchi, H., Hiwatari, K.-i., Tachikawa, H., Kimura, R., and Yamashita, S. (2010) Oligoarginine-linked polymers as a new class of penetration enhancers. *J. Controlled Release 148*, 187−196.

(27) Hayes, P. Y., Ross, B. P., Thomas, B. G., and Toth, I. (2006) Polycationic lipophilic-core dendrons as penetration enhancers for the oral administration of low molecular weight heparin. *Bioorg. Med. Chem. 14*, 143−152.

(28) Saleh, A. F., Arzumanov, A., Abes, R., Owen, D., Lebleu, B., and Gait, M. J. (2010) Synthesis and splice-redirecting activity of branched, arginine-rich peptide dendrimer conjugates of peptide nucleic acid oligonucleotides. *Bioconjugate Chem. 21*, 1902−1911.
(29) Lee, J. S., and Tung, C.-H. (2010) Lipo-oligoarginines as effective delivery vectors to promote cellular uptake. *Mol. BioSyst. 6*, 2049−2055.
(30) Pantos, A., Tsogas, I., and Paleos, C. M. (2008) Guanidinium group: A versatile moiety inducing transport and multicompartmentalization in complementary membranes. *Biochim. Biophys. Acta 1778*, 811−823.
(31) Wender, P. A., Mitchell, D. J., Pattabiraman, K., Pelkey, E. T., Steinman, L., and Rothbard, J. B. (2000) The design, synthesis, and evaluation of molecules that enable or enhance cellular uptake: Peptoid molecular transporters. *Proc.Natl. Acad. Sci. U. S. A. 97*, 13003−13008.
(32) Tyeklar, Z., Jacobson, R. R., Wei, N., Murthy, N. N., Zubieta, J., and Karlin, K. D. (1993) Reversible reaction of dioxygen (and carbon monoxide) with a copper(I) complex. X-ray structures of relevant mononuclear Cu(I) precursor adducts and the trans-(.mu.-1,2-peroxo)dicopper(II) product. *J. Am. Chem. Soc. 115*, 2677−2689.
(33) Stenzel-Rosenbaum, M. H., Davis, T. P., Chen, V., and Fane, A. G. (2001) Synthesis of poly(styrene) star polymers grown from sucrose, glucose, and cyclodextrin cores via living radical polymerization mediated by a half-metallocene iron carbonyl complex. *Macromolecules 34*, 5433−5438.
(34) Otiai, M., Hattori, T., Kitada, Y., Kuroda, H., Oyobikawa, M., Ichinomiya, S. Novel compound, polymer prepared from the compound, and composition comprising the polymer. European Patent 1156031, September 17, 2008.
(35) Sakaguchi, S. (1925) A new color reaction of protein and arginine. *J. Biochem. 5*, 25−31.
(36) Tim, M. (1983) Rapid colorimetric assay for cellular growth and survival: Application to proliferation and cytotoxicity assays. *J. Immunol. Methods 65*, 55−63.
(37) Uriel, J., Poupon, M. F., and Geuskens, M. (1983) Alphafoetoprotein uptake by cloned cell lines derived from a nickel-induced rat rhabdomyosarcoma. *Br. J. Cancer 48*, 261−9.
(38) Uriel, J., Failly-Crepin, C., Villacampa, M. J., Pineiro, A., and Geuskens, M. (1984) Incorporation of alphafetoprotein by the MCF-7 human breast cancer cell line. *Tumour Biol. 5*, 41−51.
(39) Wang, J.-S., and Matyjaszewski, K. (1995) Controlled/"living" radical polymerization. halogen atom transfer radical polymerization promoted by a Cu(I)/Cu(II) redox process. *Macromolecules 28*, 7901−7910.
(40) Kato, M., Kamigaito, M., Sawamoto, M., and Higashimura, T. (1995) Polymerization of methyl methacrylate with the carbon tetrachloride/dichlorotris- (triphenylphosphine)ruthenium(II)/methylaluminum bis(2,6-di-tert-butylphenoxide) initiating system: possibility of living radical polymerization. *Macromolecules 28*, 1721−1723.
(41) Rademacher, J. T., Baum, M., Pallack, M. E., Brittain, W. J., and Simonsick, W. J. (1999) Atom transfer radical polymerization of N,N-dimethylacrylamide. *Macromolecules 33*, 284−288.
(42) Teodorescu, M., and Matyjaszewski, K. (2000) Controlled polymerization of (meth)acrylamides by atom transfer radical polymerization. *Macromol. Rapid Commun. 21*, 190−194.
(43) Madani, F., Lindberg, S. Langel, U., Futaki, S., Gräslund, A. (2011) Mechanisms of cellular uptake of cell-penetrating peptides. *J. Biophys.*, 414729.
(44) Huang, K., Voss, B., Kumar, D., Hamm, H. E., and Harth, E. (2007) Dendritic molecular transporters provide control of delivery to intracellular compartments. *Bioconjugate Chem. 18*, 403−409.
(45) El-andaloussi, S., Järver, P., Johansson, H. J., and Langel, Ü. (2007) Cargo-dependent cytotoxicity and delivery efficacy of cell-penetrating peptides: a comparative study. *Biochem. J. 407*, 285−292.
(46) Nakase, I., Niwa, M., Takeuchi, T., Sonomura, K., Kawabata, N., Koike, Y., Takehashi, M., Tanaka, S., Ueda, K., Simpson, J. C., Jones, A. T., Sugiura, Y., and Futaki, S. (2004) Cellular uptake of arginine-rich peptides: roles for macropinocytosis and actin rearrangement. *Mol. Ther. 10*, 1011−1022.